

Research Article

Forecasting COVID-19 Cases in Egypt Using ARIMA-Based Time-Series Analysis

 Ibrahim Sabry,¹  Abdel-Hamid Ismail Mourad,^{3,4}  Amir Hussain Idrisi,³  Mohamed ElWakil²

¹Department of Manufacturing Engineering, Modern Academy for Engineering and Technology, Cairo, Egypt

²Department of Production Engineering and Mechanical Design, Faculty of Engineering, Tanta University, Tanta, Egypt

³Department of Mechanical Engineering, United Arab Emirates University, Al-Ain, United Arab Emirates

⁴On leave from Mechanical Design Department, Faculty of Engineering, Helwan University, Cairo, Egypt

Abstract

Objectives: The World Health Organization declared the novel coronavirus (COVID-19) outbreak a public health emergency of international concern on January 30, 2020. Since it was first identified, COVID-19 has infected more than one hundred million people worldwide, with more than two million fatalities. This study focuses on the interpretation of the distribution of COVID-19 in Egypt to develop an effective forecasting model that can be used as a decision-making mechanism to administer health interventions and mitigate the transmission of COVID-19.

Methods: A model was developed using the data collected by the Egyptian Ministry of Health and used it to predict possible COVID-19 cases in Egypt.

Results: Statistics obtained based on time-series and kinetic model analyses suggest that the total number of COVID-19 cases in mainland Egypt could reach 11076 per week (March 1, 2020 through January 24, 2021) and the number of simple regenerations could reach 12. Analysis of the ARIMA (2, 1, 2) and (2, 1, 3) sequences shows a rise in the number of COVID-19 events.

Conclusion: The developed forecasting model can help the government and medical personnel plan for the imminent conditions and ensure that healthcare systems are prepared to deal with them.

Keywords: ARIMA, coronavirus, COVID-19, forecast, Egypt, pandemic

Cite This Article: Sabry I, ElWakil M, Mourad AH, Idrisi AH. Forecasting COVID-19 Cases in Egypt Using ARIMA-Based Time-Series Analysis. *EJMO* 2021;5(2):123–131.

The earliest recorded pandemic occurred during the Peloponnesian War (430 BC) and may have affected as many as two-thirds of the populations of Athens, Sparta, Libya, Ethiopia, and Egypt. Over the years, the world has suffered the effects of many devastating pandemics. In addition to the effects on human physical and mental health and healthcare systems, pandemics have had significant negative effects on economies and other social and political institutions. COVID-19, the latest crippling pandemic, is still spreading worldwide. Economies have

collapsed, and the overall capabilities and fundamental values of some nations have been significantly affected. Forecasting models that estimate the number of potential new cases and deaths enable governments, healthcare providers, and healthcare systems to respond effectively. When developing reliable forecasting models, the normal progression of the disease should be considered. For an individual to contract an illness, they must be exposed to the infection. Hosts are created because of their susceptibility to infection. When more individuals come into

Address for correspondence: Abdel-Hamid Ismail Mourad, MD. Department of Mechanical Engineering, United Arab Emirates University, Al-Ain, United Arab Emirates

Phone: +971-37135116 **E-mail:** ahmourad@uaeu.ac.ae

Submitted Date: March 25, 2021 **Accepted Date:** April 29, 2021 **Available Online Date:** June 10, 2021

©Copyright 2021 by Eurasian Journal of Medicine and Oncology - Available online at www.ejmo.org

OPEN ACCESS This work is licensed under a Creative Commons Attribution-NonCommercial 4.0 International License.



contact with a contaminated host, the illness continues to spread.^[1] Basically, the carrier agent, infected hosts, and environmental factors are the three significant factors involved in the epidemiological triad. Typically, the disease transmission occurs as follows: an agent carries the pathogen, comes in contact with a host, and transfers the infection to the host under certain environmental conditions. This infection then transfers from one host to another through pathogens.^[2]

Time-series analysis is a technique for extrapolating forecasts based on a statistical model. It uses the frequency and patterns of values observed over time^[3] and, in recent years, has frequently been applied to forecast the spread of infectious diseases. For example, a time-series model has been used by several researchers to forecast the spread of measles, mumps, encephalitis B, and tuberculosis.^[4,5] With respect to time distribution, these diseases are similar to COVID-19.^[6,7] Iwendi et al.^[8] used a fine-tuned random forest model with the AdaBoost algorithm. To forecast the seriousness of a COVID-19 case and its potential outcome, i.e., recovery or mortality, this model uses the health, travel, geographical and demographic data of COVID-19-infected patients. Bayes and Valdivieso^[9] collected empirical data from China and developed a model based on a Bayesian approach to forecast the number of deaths in the next 70 days in Peru. Beck et al.^[10] employed an artificial intelligence approach to classify the commercially available medications that can be used to treat COVID-19. They suggested using the molecule transformer-drug target interaction model to establish effective treatment policies. Khalifa et al.^[11] proposed a generative adversarial network analysis with fine-tuned deep transfer learning and used 5863 chest X-ray images to detect pneumonia, which is one of the symptoms of COVID-19. Real-time predictions concerning combined cases of infectious diseases, such as pandemic influenza, Ebola, dengue, and Severe Acute Respiratory Syndrome (SARS) were established using three previously applied phenomenological methods.^[12] In a similar investigation, Yang et al.^[13] integrated the epidemiological and population migration data to train and merge the 2003 SARS model with artificial intelligence-based susceptible–exposed–infectious–delivered models to predict the COVID-19 disease curve in China. A symmetrical function was used to model the daily and cumulative number of infections, deaths, and associated significant events of the pandemic in China.^[14] Hu et al.^[15], a modified stacked automotive encoder was used to model the epidemic transmission dynamics and to predict the number of COVID-19 cases reported throughout China. To predict confirmed COVID-19 cases over the next 10 days, Al-Qaness et al.^[16] suggested com-

binning a salp swarm algorithm–enhanced flower pollination algorithm and an adaptive neuro-fuzzy inference system. In another study,^[17] simple mean-field models were utilized to forecast the expansion of COVID-19 in China, France, and Italy. In a similar study, Petropoulos and Makridakis^[18] predicted global COVID-19 cases using a simple time-series forecasting approach with an exponential smoothing model.

Herein, the Autoregressive Integrated Moving Average (ARIMA) model was used. ARIMA models are represented as ARIMA (p, d, q), where p implies the autoregression order, d is the degree of trend variance, and q is the moving average order. Furthermore, the ARIMA (2, 1, 2) model was used to estimate the occurrences of COVID-19. The strongest ARIMA model was established for our analysis relative to the predictions of other ARIMA (2, 1, 3) models and then estimated the number of cases over the next 30 days. The key purpose of this study is to identify and implement the strongest statistical model to estimate the potential occurrence of COVID-19 cases in Egypt.

Methods

Herein, data of confirmed, recovered, and fatal COVID-19 cases were collected from the Egyptian Ministry of Health's website for the period from March 1, 2020 to January 23, 2021. These data were utilized to construct forecasting models.

Model Development

ARIMA modeling is a popular computational method for predicting a time sequence with parameters p, d, and q, as previously defined. Herein, the ARIMA model was implemented using time-series data for COVID-19 cases reported in Egypt. To calculate the initial numbers of ARIMA models, partial autocorrelation function (PACF) and autocorrelation function (ACF) graphs were used. The ARIMA models were assessed for stationary and normality variances. First, they were tested for consistency by evaluating their Mean absolute percentage error (MAPE), Mean squared deviation (MSD), and Mean absolute deviation (MAD) values to determine the tuned finest expected pattern. Furthermore, the most suitable ARIMA model was compared relative to quadratic trend, linear trend, moving average, and s-curve, for single and double exponential models using a precision performance measurement, i.e., MAPE, MAD, and MSD, to select the best prediction model. The developed model was used to predict reported cases of COVID-19 for the next 30 days, i.e., from January 24, 2021 to February 24, 2021. The model used to predict reported confirmed COVID-19 cases is defined as follows:

$$ARIM(p, d, f) = a_1 X_{t-1} + a_2 X_{t-2} + B_1 Z_{t-1} + B_2 Z_{t-2} + Z_t \quad (1)$$

$$Z_t = X_t - X_{t-1} \quad (2)$$

where X_t is the estimated number of reported COVID-19 cases at the t^{th} day, model parameters are $\alpha_1, \alpha_2, \beta_1,$ and $\beta_2,$ and Z_t is the residual term for the t^{th} day.

The data of previous cases were used to forecast the trend of future occurrences using time-series analysis. Herein, time-series modeling is used to identify the patterns of reported COVID-19 cases in Egypt between March 24, 2020 and January 24, 2021, and to predict future cases between January 25, 2021 and February 24, 2021. The statistical significance value was set to 0.05. The efficiency of the model could be verified by plotting the curves for predicted and actual cases with respect to a selected time period. Furthermore, comparative analysis was performed to analyze the total number of reported COVID-19 cases in Egypt with ARIMA (2, 1, 2) and ARIMA (2, 1, 3) using the Minitab software (version 17) for all model improvements, computations, and comparisons.

Results

This study focuses on the development of a forecasting model for confirmed cases of COVID-19. The accuracies (MAPE, MSD, and MAD) listed in Table 1 show that the ARIMA (2, 1, 2) and ARIMA (2, 1, 3) models were the most reliable for the prediction of potential occurrences because they have least significant values in all scales.

Tables 2 and 3 show the estimated parameters for the ARIMA (2, 1, 3) and ARIMA (2, 1, 2) models. These tables indicate that AR (2) and MA (2) parameters are significant because the p-value is less than 0.05.

Figures 1 and 2 show the residual plots for confirmed COVID-19 cases in Egypt from January 24, 2021 to February 24, 2021, and March 1, 2020 to January 24, 2021 for ARIMA (2, 1, 3) and ARIMA (2, 1, 2), respectively.

Models	MAPE	MAD	MSD
ARIMA (2, 1, 3)	35	161	11075.8
ARIMA (2, 1, 2)	12.3	34.3	11075.8
Growth curve model	127	336	246446
Single exponential method	15.73	40.06	5519.50
Double exponential method	17.03	40.07	5595.08
Moving average (MA)	180	341	144047
S-Curve trend model	29.564	358	304917
Quadratic trend model	264	380	211852
Linear trend model	273	280	212097

MAPE: Mean absolute percentage error; MAD: Mean absolute deviation; MSD: Mean squared deviation.

Type	Coeff	SE Coeff	t	p
AR (1)	0.1730	0.0264	6.54	0.000
AR (2)	-0.9247	0.0269	-34.37	0.000
MA (1)	0.2247	0.0459	4.89	0.000
MA (2)	-0.9585	0.0058	-165.06	0.000
MA (3)	0.0472	0.0410	-1.15	0.250
Constant	3.752	7.141	0.53	0.600

SE: SE: Standard error; AR: AR: Autoregressive; MA: Moving average.

Type	Coeff	SE Coeff	t	p
AR (1)	0.1876	0.0250	7.50	0.000
AR (2)	-0.9316	0.0249	-37.39	0.000
MA (1)	0.2751	0.0175	15.76	0.000
MA (2)	-0.9822	0.0007	-1464.04	0.000
Constant	3.721	6.779	0.55	0.583

SE: SE: Standard error; AR: AR: Autoregressive; MA: Moving average.

MA (2, 1, 3) and ARIMA (2, 1, 2), respectively. The plots reveal that the residuals diverge slightly from a straight line, which indicates that the errors are fairly close to the normal plot with a few outliers. Consequently, the principle of normality is observed. This principle is confirmed by the residual histograms. A slight dispersion can be observed in the graphs plotted between the residuals and the fitted value, which indicates that the models also fulfill the assumption of constant variance. The observation order vs residual plots clearly indicate the noncorrelation of residuals.

Ljung-Box statistics for ARIMA (2, 1, 3) and ARIMA (2, 1, 2) are shown in Table 4 and Table 5, respectively. The suitability of the ARIMA (2, 1, 3) and ARIMA (2, 1, 2) models is indicated by the significance of the p-value and other statistics. PACF and ACF plots for ARIMA models (2, 1, 3) and (2, 1, 2) are shown in Figures 3 and 4, respectively. The PACF and ACF plots of confirmed cases show that the data are not stationary and have significant values at different lags. There is a constant mean in a stationary time series and no particular pattern is observed over time. However, it can satisfy the stationary condition in the mean by differentiating the original data and stationary invariance by log transformation to fit an ARIMA model.

Thus, the feasible models realized after the substitution of the predicted parameters are then determined to be ARIMA (2, 1, 3) and (2, 1, 2) models. Then, Eqs. (3) and (4) were used to predict the reported COVID-19 cases in Egypt over the next 30 days, i.e., from January 24, 2021 to February 24, 2021.

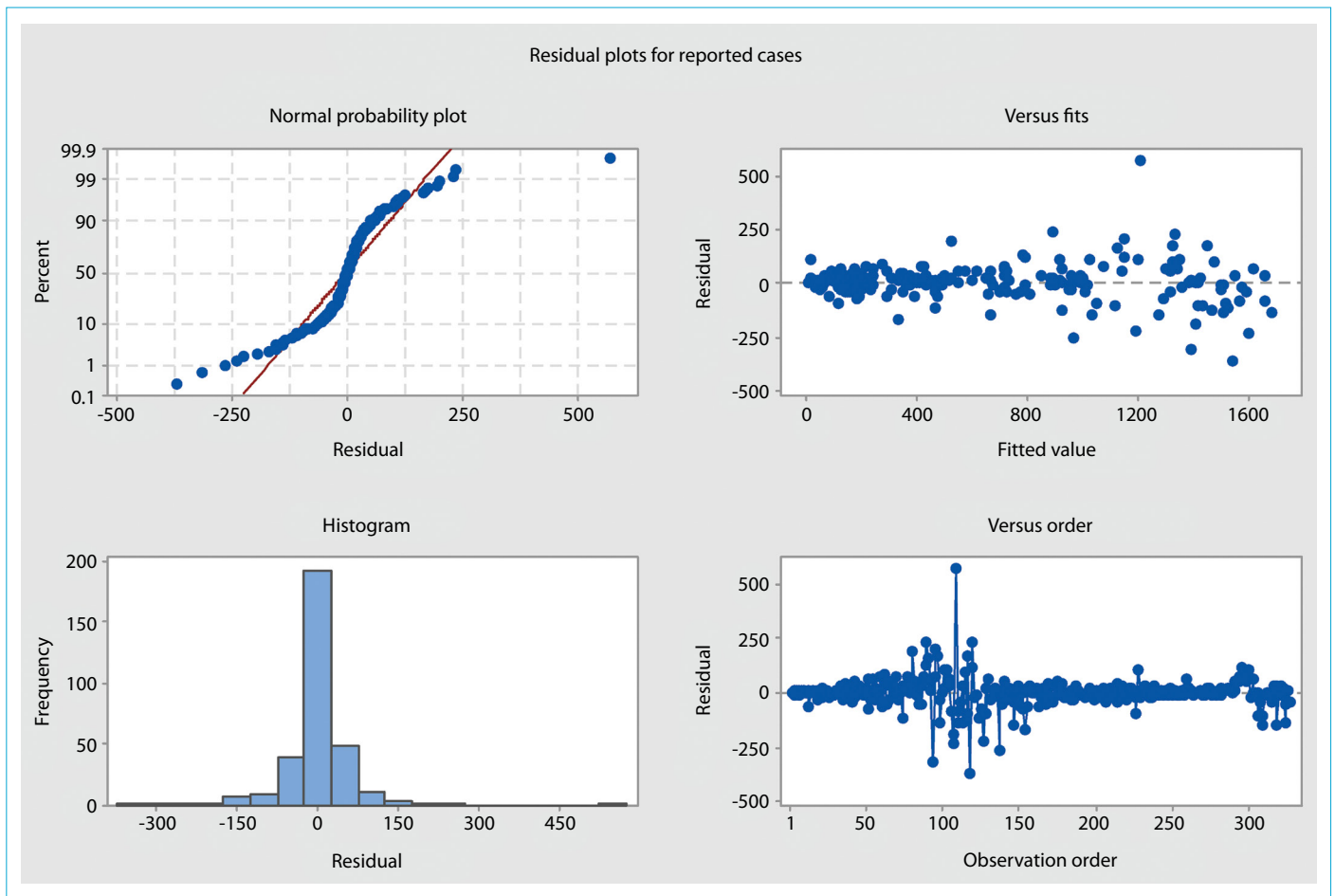


Figure 1. Residual plots ARIMA (2, 1, 3) for confirmed COVID-19 cases in Egypt from March 1, 2020 to January 24, 2021.

Table 4. Modified Box–Pierce (Ljung–Box) χ^2 statistic for ARIMA (2, 1, 3)

Lag	Chi-square	DF	p
12	30.1	6	0.000
24	54.4	18	0.000
36	61.9	36	0.000
48	71	42	0.000

DF: Degree of freedom.

Table 5. Modified Box–Pierce (Ljung–Box) χ^2 statistic for ARIMA (2, 1, 2)

Lag	Chi-square	DF	p
12	40.9	7	0.000
24	64.6	19	0.000
36	74.8	31	0.000
48	84.1	43	0.000

DF: Degree of freedom.

$$f(k) H_t = g(k) J_t \quad (3)$$

$$f(k) \nabla^d X_t = g(k) J_t \quad (4)$$

Here, $f(k)$ and $g(k)$ in Eq. (4) can be defined as follows:

$$f(k) = 1 - \alpha_1 k - \dots - \alpha_p k^p \quad (5)$$

$$g(k) = 1 - \beta_1 k - \dots - \beta_q k^q \quad (6)$$

∇^d is defined as the difference operator, which is used to make the difference of time series stationary, and d is the difference value. In real-time data, considering the first difference ($d=1$) is usually found to be sufficient, and occasionally, the second difference ($d=2$) would be sufficient to achieve stationarity.

Tables 6 and 7 describe the case prediction with a confidence interval (CI) of 95%. As per the forecast, the number of confirmed COVID-19 cases is expected to increase significantly in the following 30 days. ARIMA (2, 1, 2) was confirmed to be the optimal model based on the lowest Akaike Information Criterion (AIC) value in Eq. (7). AIC is a key criterion to select the best model among the selected models. The model with the lowest AIC value is considered the most suitable model. ACF and PACF are used to select the order of the moving average $MA(q)$ and autoregressive $AR(p)$ processes, respectively.

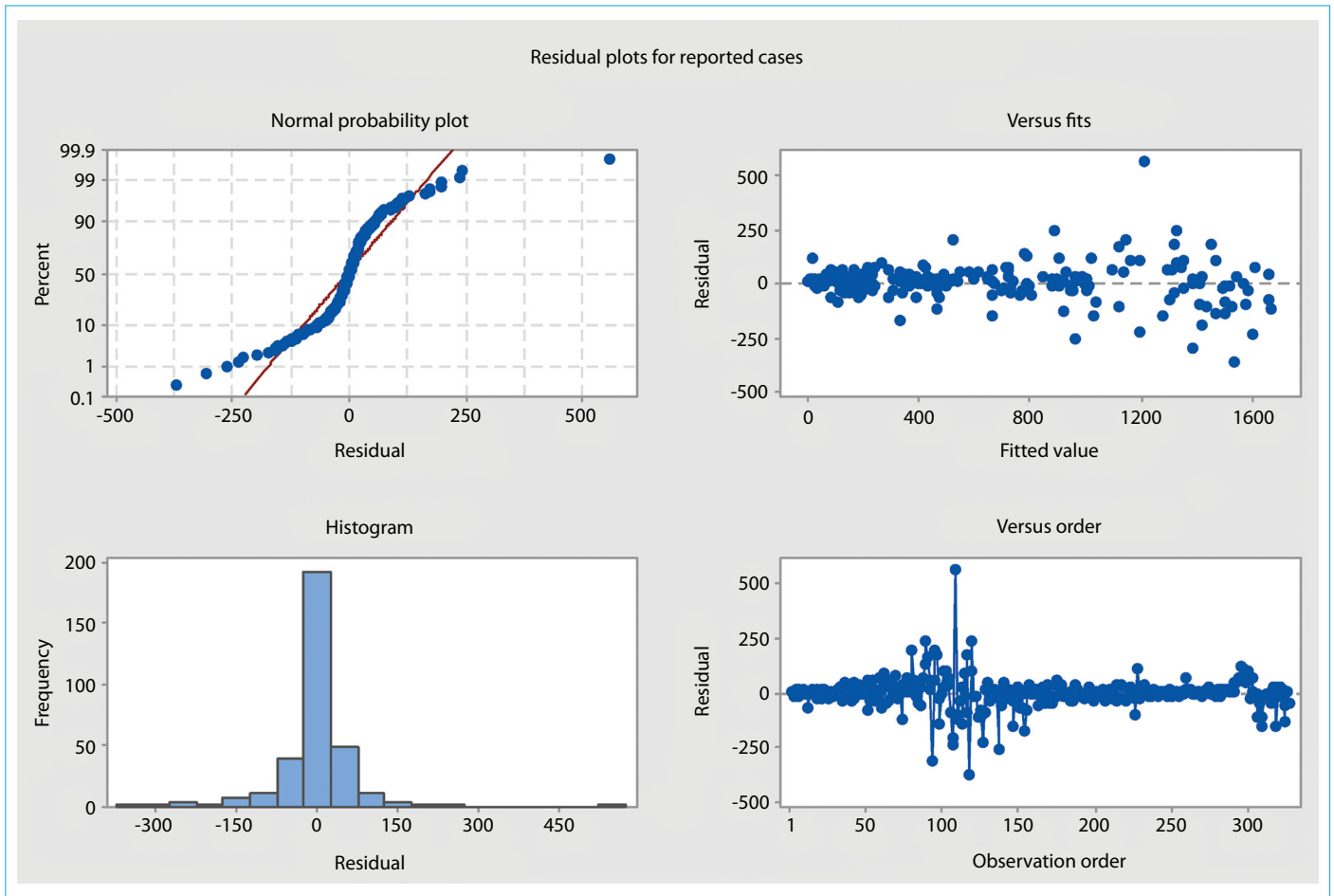


Figure 2. ARIMA (2, 1, 2) residual plots for confirmed COVID-19 cases in Egypt from March 1, 2020 to January 24, 2021.

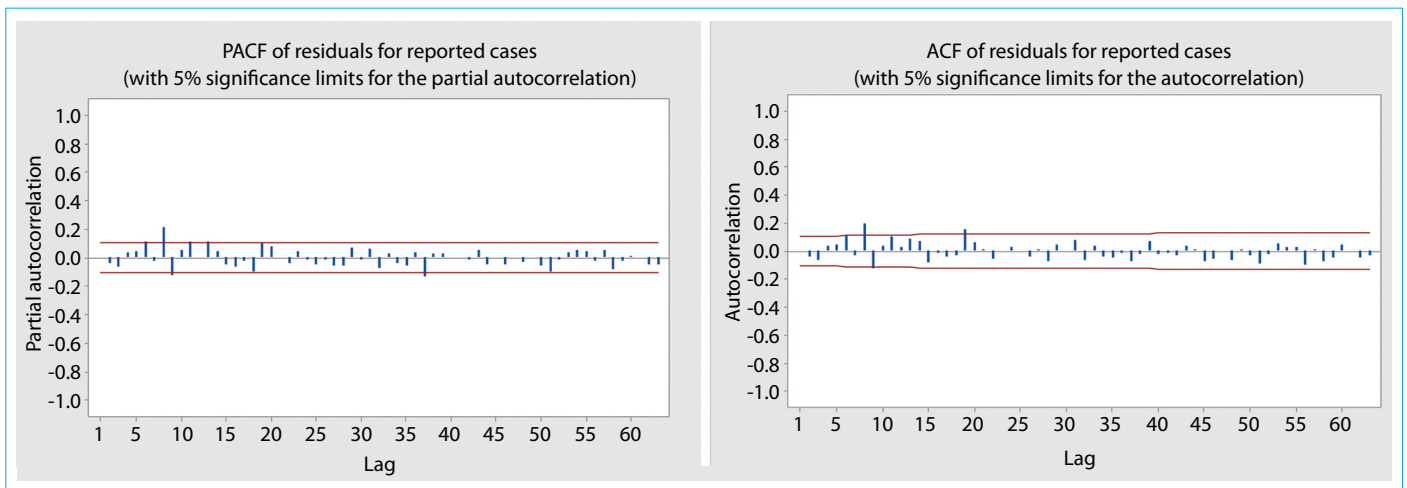


Figure 3. Residual PACF and ACF of ARIMA model (2,1,3) of cumulative confirmed cases in mainland Egypt.

$$AIC = \log \left(\frac{\sum_{t=1}^T e_t}{T} \right) + \frac{2P}{T} \quad (7)$$

The ARIMA (2, 1, 2) model was then applied to study the trend of COVID-19 from March 1, 2020 to January 24, 2021.

The model indicates that the incidents of COVID-19 cases in Egypt in this time period increased (95% confidence level of 554.19 lower limit, 839.09 upper limit, and 696.64 forecasting) as shown in Table 6. The results obtained from ARIMA models indicate a significant spread of COVID-19 infection in the subsequent days. Confirmed COVID-19 cases

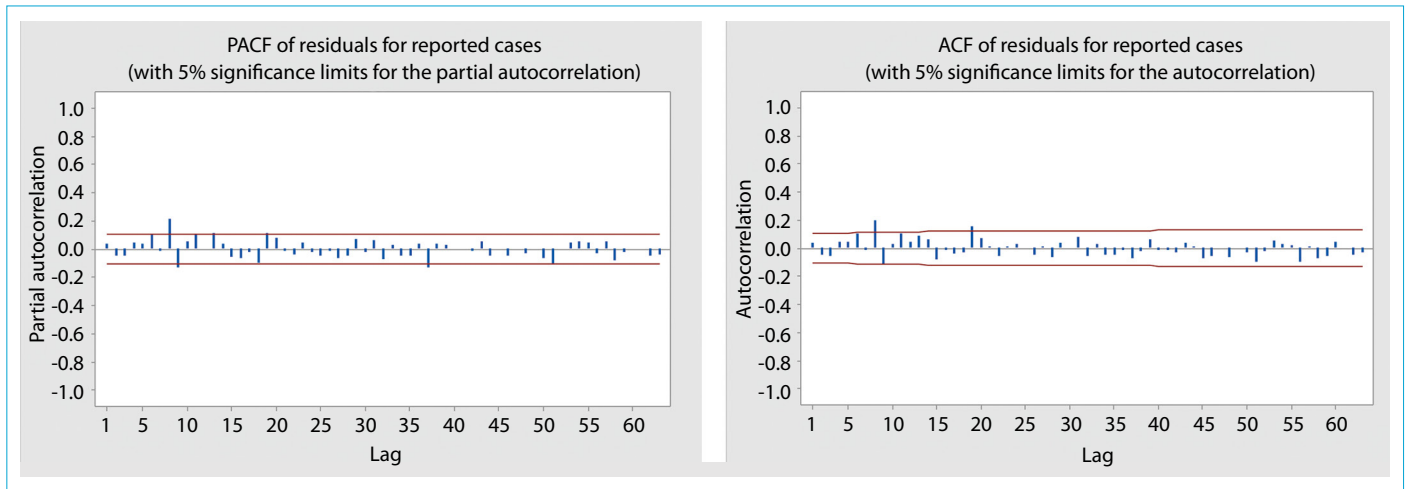


Figure 4. Residual PACF and ACF of ARIMA model (2, 1, 2) of cumulative confirmed cases in mainland Egypt.

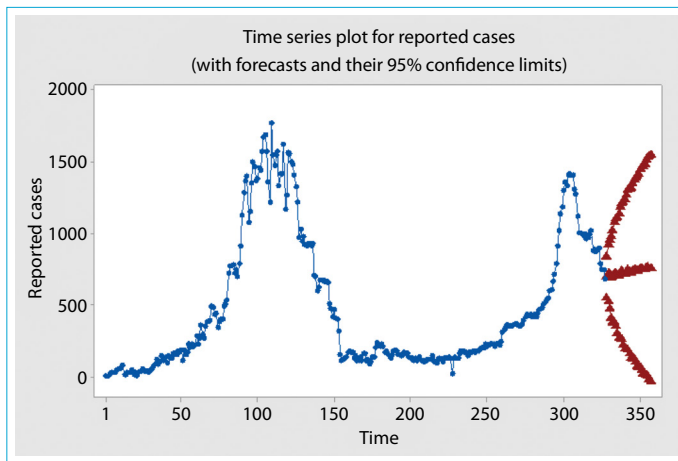


Figure 5. Time series of reported COVID-19 cases between March 1, 2020 and February 24, 2021 using ARIMA (2, 1, 3).

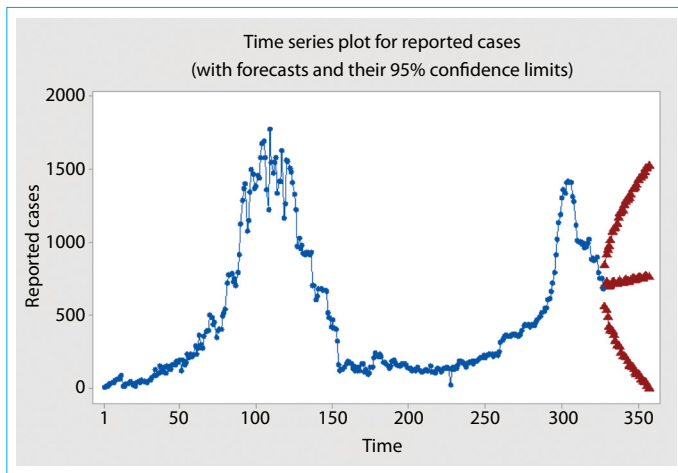


Figure 6. Time series of reported COVID-19 cases between March 1, 2020 and February 24, 2021 using ARIMA (2, 1, 2).

Table 6. ARIMA (2, 1, 3) forecast confirmed COVID-19 cases and their lower and upper limits for 30 days with a CI of 95%

Period	Forecast	Lower	Upper
328	696.64	554.19	839.09
329	723.53	527.21	919.85
330	714.42	474.09	954.75
331	691.73	406.95	976.51
332	699.98	377.2	1022.76
333	726.14	374.81	1077.47
334	726.79	349.62	1103.96
335	706.46	300.87	1112.06
336	706.1	272.73	1139.47
337	728.58	272.49	1184.68
338	736.56	260.29	1212.84
339	720.9	222.77	1219.04
340	714.57	193.72	1235.42
341	731.7	191.03	1272.38
342	744.28	186.24	1302.32
343	734.36	158.18	1310.55
344	724.77	129.18	1320.36
345	736.03	122.54	1349.53
346	750.61	121.4	1379.81
347	746.46	101.47	1391.45
348	736.02	74.03	1398.01
349	741.8	63.39	1420.21
350	756.21	63.19	1449.22
351	757.11	49.89	1464.33
352	747.7	25.32	1470.07
353	748.98	11.44	1486.52
354	761.66	10.33	1513
355	766.42	1.98	1530.85
356	759.27	-18.91	1537.44
357	757.39	-34.84	1549.62

in Egypt are expected to increase. This established model can be utilized to predict the trend of COVID-19 confirmed cases in Egypt at any time period.

Based on the lowest AIC value, it was derived that the ARIMA (2, 1, 3) model did not provide the optimal pattern.

Table 7. ARIMA (2, 1, 2) forecast confirmed COVID-19 cases and their lower and upper limits for 30 days with a CI of 95%

Period	Forecast	Lower	Upper
328	698.47	556.22	840.73
329	721.97	529.39	914.55
330	712.89	477.89	947.88
331	693.02	415.73	970.3
332	701.47	388.56	1014.37
333	725.29	385.32	1065.26
334	725.6	360.65	1090.56
335	707.19	314.9	1099.49
336	707.17	288.51	1125.83
337	728.03	287.77	1168.3
338	735.7	276.02	1195.38
339	721.41	240.67	1202.16
340	715.32	212.86	1217.77
341	731.2	209.84	1252.56
342	743.58	205.56	1281.6
343	734.83	179.36	1290.3
344	725.37	151.29	1299.46
345	735.47	144.24	1326.71
346	749.9	143.61	1356.19
347	746.92	125.49	1368.35
348	736.64	98.89	1374.39
349	741.21	87.69	1394.73
350	755.37	87.83	1422.91
351	757.49	76.35	1438.62
352	748.42	52.74	1444.09
353	748.46	38.2	1458.73
354	760.64	37.11	1484.17
355	766.61	30.53	1502.68
356	760.1	10.88	1509.32
357	757.04	-5.7	1519.79

This model was also used to research the COVID-19 occurrence pattern from March 1, 2020 to July 30, 2020. A rapid increase in COVID-19 cases in Egypt was predicted from March 1, 2020 to January 24, 2021 (95% confidence level of 556.22 lower limit, 840.73 upper limit, and 698.47 forecasting) as shown in Table 7; however, a rapid increase has not been observed and the number of predicted cases has not yet been reached. Furthermore, based on these findings, warnings must be issued about the possibility of COVID-19 spreading faster than it has been observed. Government agencies and public health authorities in Egypt can use ARIMA (2, 1, 3) model to forecast Egypt’s COVID-19 occurrence pattern.

Time-series graphs over the period between March 1, 2020 and February 24, 2021, for ARIMA (2, 1, 3) and ARIMA (2, 1, 2) are plotted in Figures 5 and 6, respectively, to compare

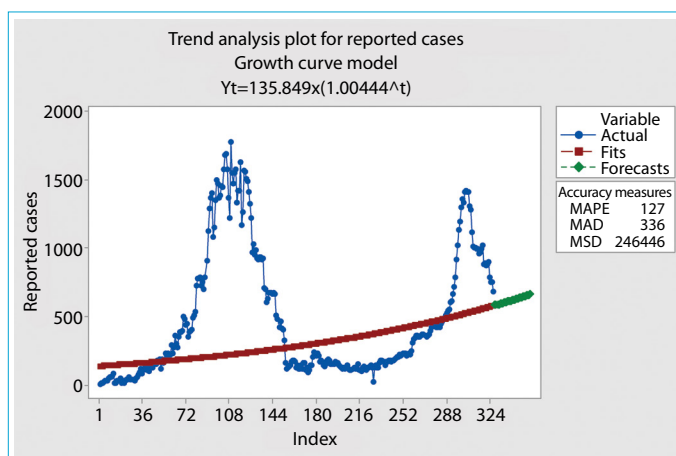


Figure 7. Comparative time-series plot for confirmed and predicted COVID-19 cases from March 1, 2020 to February 24, 2021.

the confirmed and predicted COVID-19 incidents. The correlation between predicted and real data is evident from these graphs. This comparison reveals the models’ forecasting precision. The series is not stationary. The time series reveals a growing pattern, which indicates a significant increase in COVID-19 incidents.

A time-series graph, (Fig. 7) is plotted for the time period between March 1, 2020 and February 24, 2021, to compare the actual and predicted COVID-19 cases. This plot shows the similarity between the actual and predicted data, which indicates the accuracy of the forecasting model.

Figure 8 shows the distribution plot for the reported cases. The top right portion of this plot represents the probability density function. This plot assesses the effectiveness of the distributed data points and indicates that the model is reasonable if points follow the fitted line. The Anderson–Darling statistics calculate the fit of the COVID-19 data distribution. A smaller Anderson–Darling value indicates a better data distribution fit. However, a slight difference in the values practically insignificant.

Using the alternative estimation method, i.e., the least squares (LSXY) method, the Minitab software displays a Pearson correlation coefficient for COVID-19. This correlation coefficient must be positive but not greater than 1. In addition, the distribution provides a better fit if the correlation coefficient values are high.

Figure 9 shows the time series plot of confirmed COVID-19 cases of Egypt. This plot indicates that the number of cases could be controlled in a few days by following strict preventive measures, such as sanitization and quarantine.

Conclusion

COVID-19 is a significant global threat that was declared a pandemic by the Egyptian Health Ministry. This study aimed

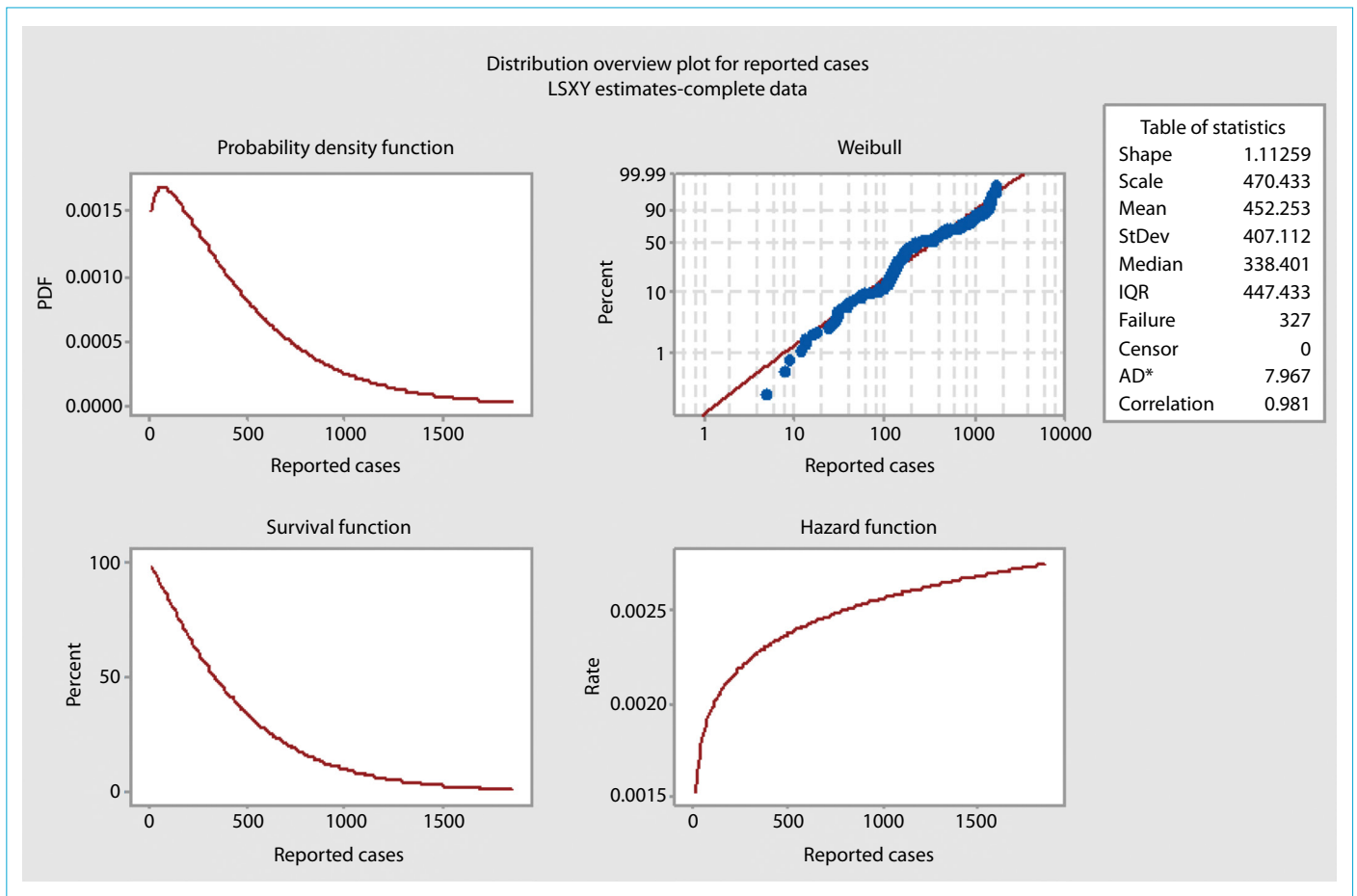


Figure 8. Distribution overview plot.

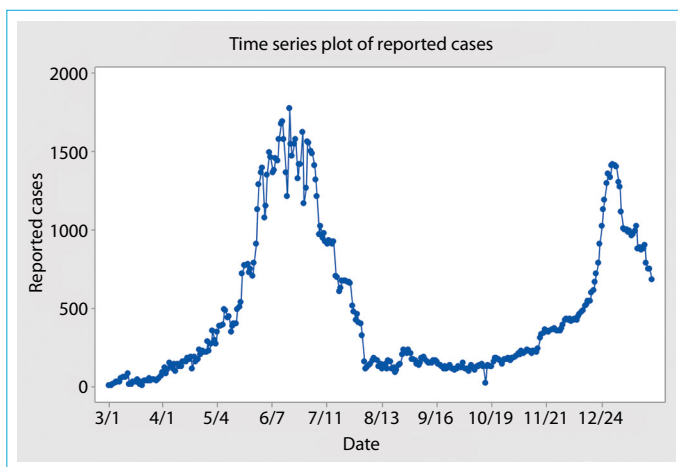


Figure 9. Time series plot of reported COVID-19 cases.

to determine the best model for forecasting COVID-19 cases. The model was used to estimate the possible cases of COVID-19 infection in Egypt and is expected to be applied to promote disease control and help in the planning of healthcare services. The reported cases are predicted to increase in the coming days according to the model forecast. The time series analysis indicates an exponential increase

in COVID-19 infections. However, it is expected that measures, such as social distancing, lockdown etc., may impact this forecast, and cases may continue to increase after approximately one month.

Disclosures

Ethics Committee Approval: Ethics committee approval was not requested for this study.

Peer-review: Externally peer-reviewed.

Conflict of Interest: None declared.

Authorship Contributions: Concept – I.S., M.E., A-H.I.M.; Design – I.S., M.E., A.H.I.; Supervision – I.S., A-H.I.M.; Materials – I.S., M.E., A-H.I.M.; Data collection &/or processing – I.S., A.H.I.; Analysis and/or interpretation – A.H.I., A-H.I.M.; Literature search – M.E., A.H.I.; Writing – I.S., A.H.I.; Critical review – M.E., A-H.I.M.

References

1. Maier BF, Brockmann D. Effective containment explains sub-exponential growth in recent confirmed COVID-19 cases in China. *Science* 2020;368:742–6.
2. Luz PM, Mendes BV, Codeço CT, Struchiner CJ, Galvani AP. Time series analysis of dengue incidence in Rio de Janeiro,

- Brazil. *Am J Trop Med Hyg* 2008;79:933–9.
3. Woo PC, Huang Y, Lau SK, Yuen KY. Coronavirus genomics and bioinformatics analysis. *Viruses* 2010;2:1804–20.
 4. Allard R. Use of time-series analysis in infectious disease surveillance. *Bull World Health Organ* 1998;76:327.
 5. Wu JB, Ye LX, You EK. Prediction of incidence of notifiable contagious diseases by application of time series model. *Math Med Biol* 2007;1:90–2.
 6. WHO. Coronavirus disease 2019 (COVID-19): situation report, 82. Available at: <https://apps.who.int/iris/handle/10665/331780>. Accessed May 21, 2021.
 7. Sahin AR, Erdogan A, Agaoglu PM, Dineri Y, Cakirci AY, Senel ME, et al. 2019 novel coronavirus (COVID-19) outbreak: a review of the current literature. *EJMO* 2020;4:1–7.
 8. Iwendi C, Bashir AK, Peshkar A, Sujatha R, Chatterjee JM, Pasupuleti S, et al. COVID-19 patient health prediction using boosted random forest algorithm. *Front Public Health* 2020;8:357.
 9. Bayes C, Sal y Rosas V, Valdivieso L. Modelling death rates due to COVID-19: A Bayesian approach. *Cornell University arXiv:2004.02386*.
 10. Beck BR, Shin B, Choi Y, Park S, Kang K. Predicting commercially available antiviral drugs that may act on the novel coronavirus (SARS-CoV-2) through a drug-target interaction deep learning model. *Comput Struct Biotechnol J* 2020;18:784–90.
 11. Khalifa NEM, Taha MHN, Hassanien AE, Elghamrawy S. Detection of coronavirus (covid-19) associated pneumonia based on generative adversarial networks and a fine-tuned deep transfer learning model using chest x-ray dataset. *Cornell University arXiv:2004.01184*.
 12. Roosa K, Lee Y, Luo R, Kirpich A, Rothenberg R, Hyman JM, et al. Real-time forecasts of the COVID-19 epidemic in China from February 5th to February 24th, 2020. *Infect Dis Model* 2020;5:256–63.
 13. Yang Z, Zeng Z, Wang K, Wong SS, Liang W, Zanin M, et al. Modified SEIR and AI prediction of the epidemics trend of COVID-19 in China under public health interventions. *J Thorac Dis* 2020;12:165–74.
 14. Li Q, Feng W, Quan YH. Trend and forecasting of the COVID-19 outbreak in China. *J Infect* 2020;80:469–96.
 15. Hu Z, Ge Q, Li S, Jin L, Xiong M. Artificial intelligence forecasting of covid-19 in China. *Cornell University arXiv:2002.07112*.
 16. Al-Qaness MAA, Ewees AA, Fan H, Abd El Aziz M. Optimization Method for Forecasting Confirmed Cases of COVID-19 in China. *J Clin Med* 2020;9:674.
 17. Fanelli D, Piazza F. Analysis and forecast of COVID-19 spreading in China, Italy and France. *Chaos Solitons Fractals* 2020;134:109761
 18. Petropoulos F, Makridakis S. Forecasting the novel coronavirus COVID-19. *PLoS One* 2020;15:e0231236.